

## Electromagnetic Response of $^{12}\text{C}$ : A First-Principles Calculation

A. Lovato,<sup>1</sup> S. Gandolfi,<sup>2</sup> J. Carlson,<sup>2</sup> Steven C. Pieper,<sup>1</sup> and R. Schiavilla<sup>3,4</sup>

<sup>1</sup>*Physics Division, Argonne National Laboratory, Argonne, Illinois 60439, USA*

<sup>2</sup>*Theoretical Division, Los Alamos National Laboratory, Los Alamos, New Mexico 87545, USA*

<sup>3</sup>*Theory Center, Jefferson Lab, Newport News, Virginia 23606, USA*

<sup>4</sup>*Department of Physics, Old Dominion University, Norfolk, Virginia 23529, USA*

(Received 6 May 2016; revised manuscript received 6 July 2016; published 15 August 2016)

The longitudinal and transverse electromagnetic response functions of  $^{12}\text{C}$  are computed in a “first-principles” Green’s function Monte Carlo calculation, based on realistic two- and three-nucleon interactions and associated one- and two-body currents. We find excellent agreement between theory and experiment and, in particular, no evidence for the quenching of the measured versus calculated longitudinal response. This is further corroborated by a reanalysis of the Coulomb sum rule, in which the contributions from the low-lying  $J^\pi = 2^+, 0_2^+$  (Hoyle), and  $4^+$  states in  $^{12}\text{C}$  are accounted for explicitly in evaluating the total inelastic strength.

DOI: 10.1103/PhysRevLett.117.082501

One of the challenges in quantum many-body physics is calculating the electroweak response of a nucleus by fully accounting for the dynamics of its constituent nucleons. In this Letter we report the first such calculation for the electromagnetic response of the  $^{12}\text{C}$  nucleus.

The nucleons interact with each other via two- and three-body forces and with external electroweak fields via one- and two-body, and smaller many-body, currents. This dynamical picture of the nucleus in which the consequences of the nucleons’ substructure on its structure and response are subsumed into effective many-body forces and currents is by now well established. When coupled to numerically exact methods, such as the Green’s function Monte Carlo (GFMC) methods adopted in this work, it has led to a quantitative and successful “first-principles” understanding of many nuclear properties including the low-lying energy spectra of nuclei up to  $^{12}\text{C}$  (Ref. [1] and references therein), their radii and magnetic moments [2,3], their elastic and inelastic electromagnetic form factors [4,5], electroweak transitions between their low-lying states ( $M1$  and  $E2$  widths [2,3], and  $\beta$ -decay and electron-capture rates [6]), and properties of their ground-state structure, such as the momentum distributions of nucleons and nucleon pairs [7], and insights into the role that the dominant features of the nuclear interaction—the short-range repulsion and long-range tensor nature—have in shaping their ground-state structure [8], and more (for a recent review see Ref. [1]). One of the key features of this approach is the assumption that the couplings of the external fields to the nucleons are governed by those in free space with modifications induced primarily by two-nucleon currents. However, it should be emphasized that the GFMC method, as presently formulated, cannot account for explicit  $\pi$ -production processes; in particular, it is not suitable to describe the  $\Delta$ -excitation peak region.

Here, we report calculations of the  $^{12}\text{C}$  electromagnetic longitudinal and transverse response functions, denoted, respectively, as  $R_L(q, \omega)$  and  $R_T(q, \omega)$ , where  $q$  and  $\omega$  are the electron momentum and energy transfers. These response functions are obtained experimentally by the Rosenbluth separation of inclusive  $(e, e')$  scattering data [9,10]. The calculations are based on the AV18 + IL7 combination of two- and three-nucleon potentials [11,12] and the accompanying set of two-body electromagnetic currents (for a review see Ref. [1] and references therein). GFMC methods are used to compute these responses as functions of imaginary time [13,14], and maximum-entropy techniques to infer from these imaginary-time data the actual  $R_L(q, \omega)$  and  $R_T(q, \omega)$  [15–17]. These latter two aspects of this study are discussed below.

Accurate calculations of the nuclear response are necessary to reliably test this realistic framework of nuclear dynamics. In simplified approaches, for example, an increase in nucleon size has been advocated to explain the depletion of the nuclear structure functions measured by deep inelastic scattering (the European Muon Collaboration (EMC) effect [18]), the quenching of the quasielastic longitudinal response measured in  $(e, e')$  scattering off light and heavy nuclear targets [19,20], and the suppression in the ratio of transverse to longitudinal polarization transfers in  $^4\text{He}$  relative to the ratio in hydrogen, measured via the  $^4\text{He}(\vec{e}, e'\vec{p})^3\text{H}$  reaction at quasielastic kinematics at Jefferson Lab (Ref. [21] and references therein).

Clearly, the question of in-medium modifications is model dependent. Indeed, theoretical approaches based on the realistic picture outlined above indicate that binding and correlation effects, included by employing realistic spectral functions, lead to average removal energies much larger than those adopted in standard EMC calculations, and provide a quantitative account of both the size and density dependence of the EMC effect [22–24].

Such approaches also show that spin-dependent final state interaction effects and corrections beyond the impulse approximation, induced by two-body electromagnetic currents, resolve the discrepancy between theory and experiment in the case of the polarization-transfer ratio when the free nucleon electromagnetic form factors are used in the nuclear currents [25].

The quark-meson coupling approach, which attempts to self-consistently account for nucleon and nuclear structure [26,27], leads to a reduction of the proton electric form factor, and, as a consequence, to a significant quenching of the longitudinal response function of nuclear matter and the associated Coulomb sum rule [20]. Such a model does not explain the large enhancement of the transverse response or the momentum-transfer dependence in the quenching of the longitudinal one. It should also be noted that medium modifications are not an inevitable consequence of the quark substructure of the nucleon. For example, a study of the two-nucleon problem in a flux-tube model of six quarks interacting via single gluon and pion exchanges [28] indicates that the nucleons retain their individual identities down to very short separations, with little distortion of their substructures.

In this Letter we show that accurate calculations of the response based on a realistic correlated nuclear wave function and containing one- and two-body currents with free nucleon form factors can completely reproduce the  $^{12}\text{C}$  longitudinal and transverse electromagnetic response below the delta resonance.

The longitudinal and transverse response functions are defined as

$$R_\gamma(q, \omega) = \sum_f \langle f | j_\gamma(\mathbf{q}, \omega) | 0 \rangle \langle f | j_\gamma(\mathbf{q}, \omega) | 0 \rangle^* \times \delta(E_f - \omega - E_0), \quad \gamma = L, T, \quad (1)$$

where  $|0\rangle$  and  $|f\rangle$  represent the nuclear initial and final states of energies  $E_0$  and  $E_f$ , and  $j_L(\mathbf{q}, \omega)$  and  $j_T(\mathbf{q}, \omega)$  are the electromagnetic charge and current operators, respectively. A direct calculation of  $R_\gamma(q, \omega)$  is impractical, because it would require evaluating each individual transition amplitude  $|0\rangle \rightarrow |f\rangle$  induced by the charge and current operators. To circumvent this difficulty, the use of integral transform techniques has proved to be quite helpful. One such approach is based on the Laplace transform of  $R_\gamma(q, \omega)$ —i.e., the Euclidean response [13] defined as

$$E_\gamma(q, \tau) = \int_{\omega_{\text{el}}^+}^{\infty} d\omega e^{-\omega\tau} \frac{R_\gamma(q, \omega)}{[G_E^p(q, \omega)]^2}, \quad (2)$$

where  $G_E^p(q, \omega)$  is the (free) proton electric form factor and the integration excludes the contribution due to elastic scattering ( $\omega_{\text{el}}$  is the energy of the recoiling ground state). We elaborate this issue further below; for now it suffices to note that, in the specific case of  $^{12}\text{C}$ , the ground state has quantum numbers  $J^\pi = 0^+$  and therefore the elastic contribution vanishes in the transverse channel. With the

definition given in Eq. (2), the Euclidean response function above can be thought of as being due to pointlike, but strongly interacting, nucleons, and can simply be expressed as

$$E_\gamma(q, \tau) = \langle 0 | O_\gamma^\dagger(\mathbf{q}) e^{-(H-E_0)\tau} O_\gamma(\mathbf{q}) | 0 \rangle - |F_\gamma(q)|^2 e^{-\tau\omega_{\text{el}}}, \quad (3)$$

where  $H$  is the nuclear Hamiltonian (here, the AV18 + IL7 model),  $F_\gamma(q) = \langle 0 | O_\gamma(\mathbf{q}) | 0 \rangle$  is the elastic form factor, and in the electromagnetic operators  $O_\gamma(\mathbf{q})$  the dependence on the energy transfer  $\omega$  has been removed by dividing the current  $j_\gamma(\mathbf{q}, \omega)$  by  $G_E^p(q, \omega)$  [17]. The calculation of this matrix element is then carried out with GFMC methods [13] similar to those used in projecting out the exact ground state of  $H$  from a trial state [29]. It proceeds in two steps. First, an unconstrained imaginary-time propagation of the state  $|0\rangle$  is performed and saved. Next, the states  $O_\gamma(\mathbf{q})|0\rangle$  are evolved in imaginary time following the path previously saved. During this latter imaginary-time evolution, scalar products of  $\exp[-(H-E_0)\tau_i] O_\gamma(\mathbf{q})|0\rangle$  with  $O_\gamma(\mathbf{q})|0\rangle$  are evaluated on a grid of  $\tau_i$  values, and from these scalar products estimates for  $E_\gamma(q, \tau_i)$  are obtained (a complete discussion of the methods is in Refs. [13,30]). We use our best variational trial wave function  $\Psi_T$  for  $|0\rangle$  and thus the response functions are those of  $\Psi_T$  instead of the evolved GFMC wave function. The sum rule results of Ref. [5] indicate that for the momentum transfers we consider and for  $\omega$  in the quasielastic peak region, the accuracy of this approximation is at the few percent level.

Following Ref. [17] (see also the extended material submitted in support of that publication), we have exploited maximum entropy techniques [15,16] to perform the analytic continuation of the Euclidean response—corresponding to the inversion of the Laplace transform of Eq. (2). However, we have improved on the inversion procedure described in Ref. [17] in order to better propagate the statistical errors associated with  $E_\gamma(q, \tau)$  into  $R_\gamma(q, \omega)$ . Specifically, the smallest possible value for the parameter  $\alpha$  (see Ref. [17]) of the maximum entropy algorithm has been chosen to perform a first inversion of the Laplace transform, which is then independent of the prior. The resulting response function  $R^{(0)}$  is the one whose Laplace transform  $E^{(0)}$  is the closest to the original average GFMC Euclidean response. Then, 100 Euclidean response functions are sampled from a multivariate Gaussian distribution, with the mean value  $E^{(0)}$  and covariance estimated from the original set of GFMC Euclidean responses. The corresponding response functions, obtained using the so called “historic maximum entropy” technique [16], are used to estimate the mean value and the variance of the final inverted response function.

We now proceed to address the issue of excluding the elastic contribution. The low-lying excitation spectrum of  $^{12}\text{C}$  consists of  $J^\pi = 2^+$ ,  $0_2^+$  (Hoyle), and  $4^+$  states with

TABLE I. Measured longitudinal transition form factors, defined as  $\langle f|O_L(\mathbf{q})|0\rangle/Z$ , to the  $f = 2^+, 0_2^+$  (Hoyle), and  $4^+$  states in  $^{12}\text{C}$ . Experimental data are from Refs. [32–34], and have been divided by the proton electric form factor  $G_E^p(q, \omega_f)$  with  $\omega_f = E_f - E_0$ , as described in Ref. [35].

| $q$ (MeV/c) | $2^+$  | $0_2^+$ | $4^+$   |
|-------------|--------|---------|---------|
| 300         | 0.128  | 0.0313  | 0.0010  |
| 380         | 0.0743 | 0.0052  | 0.0012  |
| 570         | 0.0043 | 0.0045  | 0.00059 |

excitation energies  $E_f^* - E_0$  experimentally known to be, respectively, 4.44, 7.65, and 14.08 in MeV units [31]. The contributions of these states to the quasielastic longitudinal and transverse response functions extracted from inclusive ( $e, e'$ ) cross section measurements are not included in the experimental results. Therefore, before comparing experiment with the present theory, which computes the total inelastic response rather than just the quasielastic one, we need to remove these contributions explicitly. This is simply accomplished by first defining

$$\bar{E}_\gamma(q, \tau) = E_\gamma(q, \tau) - \sum_f |\langle f|O_\gamma(\mathbf{q})|0\rangle|^2 e^{-(E_f - E_0)/\tau}, \quad (4)$$

where in the sum only the states  $f = 2^+, 0_2^+$ , and  $4^+$  are included, and then inverting  $\bar{E}(q, \tau)$  (the energies  $E_f$  differ from  $E_f^*$ , since the former include recoil kinetic energies). We do not attempt a GFMC calculation of the excitation energies of these states or associated transition form factors—it would require explicit calculations of these states or propagating  $\exp[-(H - E_0)\tau]O_\gamma(\mathbf{q})|0\rangle$  to computationally prohibitive large values of  $\tau$ . Rather, we use the experimental energies and form factors, listed in Table I, to obtain  $\bar{E}_\gamma(q, \tau)$  from the GFMC-calculated  $E_\gamma(q, \tau)$ . Because of the fast drop of these form factors with increasing momentum transfer, the correction in Eq. (4) for the longitudinal channel ( $\gamma = L$ ) is significant at  $q = 300$  MeV/c, but completely negligible at  $q = 570$  MeV/c. In the case of the transverse channel ( $\gamma = T$ ), possible contributions from  $E2$  and  $E4$  transitions to the  $2^+$  and  $4^+$  states are too small [40,41] to have an impact on  $\bar{E}_T(q, \tau)$ .

The longitudinal and transverse response functions obtained by the maximum-entropy inversion of the  $\bar{E}_\gamma(q, \tau)$ 's are displayed in Figs. 1 and 2, respectively. Theoretical predictions corresponding to GFMC calculations in which only one-body terms or both one- and two-body terms are retained in the electromagnetic operators  $O_\gamma$ —denoted by (red) dashed and (black) solid lines and labeled GFMC  $O_{1b}$  and GFMC  $O_{1b+2b}$ , respectively—are compared to the experimental response functions determined from the world data analysis of Jourdan [10] and, for  $q = 300$  MeV/c, from the Saclay data [9]. The (red and gray) shaded areas show the uncertainty derived from the dependence of the  $1b$  and  $1b + 2b$  results on the default

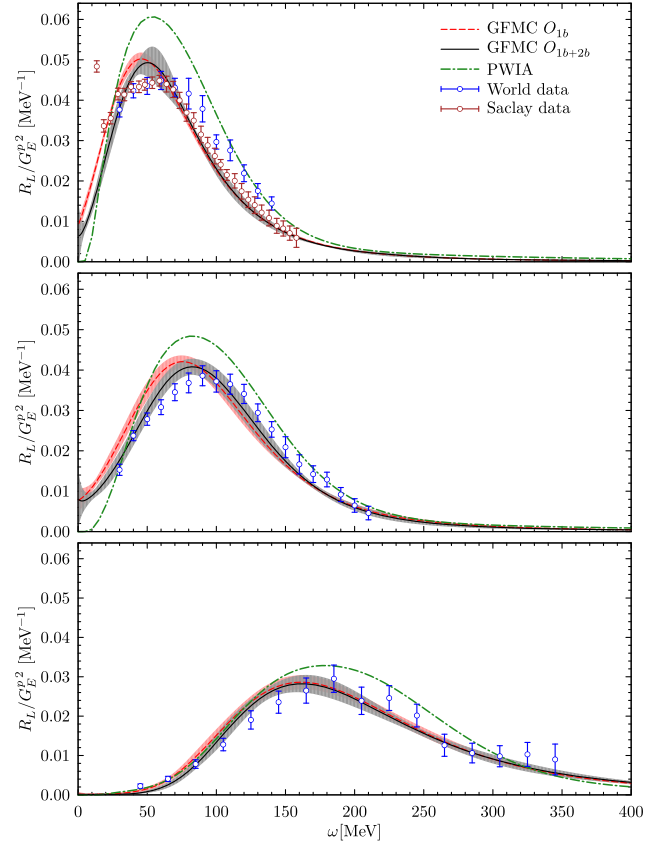


FIG. 1. Electromagnetic longitudinal response functions of  $^{12}\text{C}$  for  $q$  in the range 300–570 MeV. Experimental data are from Refs. [9,10]. See the text for further explanations.

model adopted in the maximum-entropy inversion [17]. This uncertainty is quite small. Lastly, the (green) dash-dotted lines correspond to plane-wave-impulse-approximation (PWIA) calculations using the single-nucleon momentum distribution  $N(p)$  of  $^{12}\text{C}$  obtained in Ref. [7] (see Ref. [1] for details on the PWIA calculation).

Figures 1 and 2 immediately lead to the main conclusions of this work: (i) the dynamical approach outlined above (with free nucleon electromagnetic form factors) is in excellent agreement with experiment in both the longitudinal and transverse channels, (ii) as illustrated by the difference between the PWIA and GFMC one-body-current predictions (curves labeled PWIA and GFMC  $O_{1b}$ ), correlations and interaction effects in the final states redistribute strength from the quasielastic peak to the threshold and high-energy transfer regions, and (iii) while the contributions from two-body charge operators tend to slightly reduce  $R_L(q, \omega)$  in the threshold region, those from two-body currents generate a large excess of strength in  $R_T(q, \omega)$  over the whole  $\omega$  spectrum (curves labeled GFMC  $O_{1b}$  and GFMC  $O_{1b+2b}$ ), thus offsetting the quenching noted in (ii) in the quasielastic peak.

As a result of this study, a consistent picture of the electromagnetic response of nuclei emerges, which is at variance with the conventional one of quasielastic

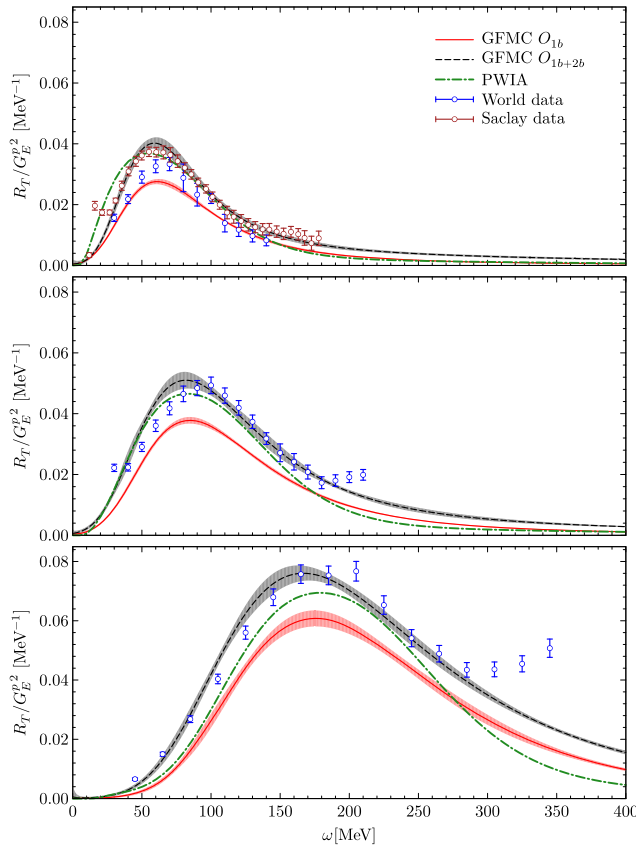


FIG. 2. Same as Fig. 1 but for the electromagnetic transverse response functions. Because pion production mechanisms are not included, the present theory underestimates the (transverse) strength in the  $\Delta$  peak region; see in particular the  $q = 570$  MeV/ $c$  case.

scattering as being dominated by a single-nucleon knock out. This fact also has implications for the nuclear weak response probed in inclusive neutrino scattering induced by charge-changing and neutral current processes. In particular, the energy dependence of the cross section is quite important in extracting neutrino oscillation parameters. An earlier study of the sum rules associated with the weak transverse and vector-axial interference response functions in  $^{12}\text{C}$  found [42] a large enhancement due to two-body currents in both the vector and axial components of the neutral current. Only neutral weak processes have been considered so far, but one would expect these conclusions to remain valid in the case of charge-changing ones. In this connection, it is important to realize that neutrino and antineutrino cross sections differ only in the sign of this vector-axial interference response, and that this difference is crucial for inferring the charge-conjugation and parity violating phase, one of the fundamental parameters of neutrino physics, to be measured at the Deep Underground Neutrino Experiment (DUNE)[43].

We conclude by updating in Fig. 3 the results for the Coulomb sum rule of  $^{12}\text{C}$  obtained in Ref. [5]. The theoretical calculation (solid line) is identical to the one

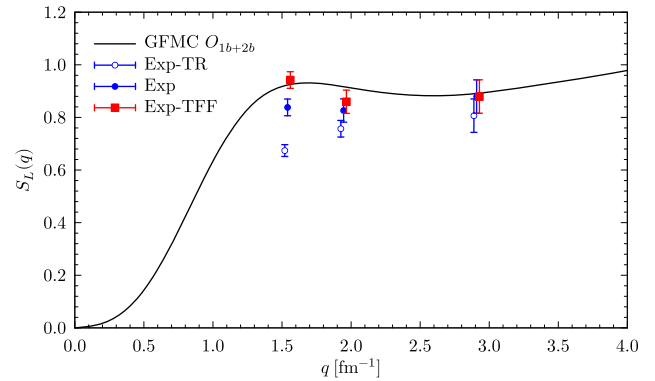


FIG. 3. Coulomb sum rule in  $^{12}\text{C}$ : theory (black solid line labeled  $1b + 2b$ ) and analyses of experimental data (blue empty and full circles labeled EXP-TR and EXP) are from Ref. [5]; the (red square) data points, labeled EXP-TFF, include the contributions of the low-lying  $J^\pi = 2^+, 0_2^+$  (Hoyle), and  $4^+$  states; see the text for explanations.

reported in that work. In the present analysis of the experimental data (empty and full circles), the inelastic threshold has been assumed to correspond to the energy of the  $4^+$  state rather than to that of the  $2^+$  state, as we have explicitly accounted for the transitions to the low-lying states. We recall that the empty circles are obtained by integrating  $R_L(q, \omega)$  up to  $\omega_{\text{max}}$ , the highest measured energy transfer, while the full circles also include the “tail” contribution for  $\omega > \omega_{\text{max}}$  and into the timelike region ( $\omega > q$ ), which cannot be accessed in  $(e, e')$  scattering experiments, by assuming that the longitudinal response in  $^{12}\text{C}$  is proportional to that of the deuteron [5]. As the direct calculations demonstrate in Figs. 1 and 2, there is non-vanishing strength in the timelike region (see in particular the top panels of these figures which extend to  $\omega > q$ ), and this strength needs to be accounted for before comparing theory to experiment.

The square data points in Fig. 3 have been obtained by adding to the full circles the contribution due to the low-lying  $J^\pi = 2^+, 0_2^+$ , and  $4^+$  states. Given the choice of normalization for  $S_L(q)$  in Fig. 3, this contribution is simply given by the sum of the squares—each multiplied by  $Z = 6$ —of the (longitudinal) transition form factors listed in Table I. Among these, the dominant one is the form factor to the  $2^+$  state at a 4.44 MeV excitation energy. The contributions associated with these states, in particular the  $2^+$  state, were overlooked in the analysis of Ref. [5] and, to the best of our knowledge, in all preceding analyses—the difference between the total inelastic and quasielastic strength alluded to earlier was not fully appreciated. While they are negligible at large  $q$  (certainly at  $q = 570$  MeV/ $c$ ), they are significant at low  $q$ . They help to bring theory into excellent agreement with experiment.

Figures 1 and 2 clearly demonstrate that the picture of interacting nucleons and currents quantitatively describes the electromagnetic response of  $^{12}\text{C}$  in the quasielastic regime. The key features necessary for this successful

description are a complete and consistent treatment of initial-state correlations and final-state interactions and a realistic treatment of two-nucleon currents, all fully and exactly accounted for in the GFMC calculations. In the transverse channel the interference between one- and two-body current (schematically,  $1b$  and  $2b$ ) contributions is largely responsible for enhancement in the quasielastic peak, while this interference plays a minor role at large  $\omega$ , where  $2b$ - $2b$  contributions become dominant. The absence of explicit pion production mechanisms in this channel restricts the applicability of the present theory to the quasielastic region of  $R_T(q, \omega)$ , for  $\omega$ 's below the  $\Delta$ -resonance peak. Finally, the so-called quenching of the longitudinal response near the quasielastic peak emerges in this study as a result of initial-state correlations and final-state interactions.

A critical reading of the manuscript by Ingo Sick is gratefully acknowledged. We also thank P. von Neumann-Cosel for providing us with the data on the form factor for the transition from the ground state in  $^{12}\text{C}$  to the Hoyle state. This research is supported by the U.S. Department of Energy, Office of Science, Office of Nuclear Physics, under Contracts No. DE-AC02-06CH11357 (A. L. and S. C. P.), No. DE-AC52-06NA25396 (S. G. and J. C.), and No. DE-AC05-06OR23177 (R. S.), and by the NUCLEI SciDAC and LANL LDRD programs. Under an award of computer time provided by the INCITE program, this research used resources of the Argonne Leadership Computing Facility at Argonne National Laboratory, which is supported by the Office of Science of the U.S. Department of Energy under Contract No. DE-AC02-06CH11357. It also used resources provided by Los Alamos Open Supercomputing, by Argonne LCRC, and by the National Energy Research Scientific Computing Center, which is supported by the Office of Science of the U.S. Department of Energy under Contract No. DE-AC02-05CH11231.

---

[1] J. Carlson, S. Gandolfi, F. Pederiva, S. C. Pieper, R. Schiavilla, K. E. Schmidt, and R. B. Wiringa, *Rev. Mod. Phys.* **87**, 1067 (2015).  
 [2] S. Pastore, S. C. Pieper, R. Schiavilla, and R. B. Wiringa, *Phys. Rev. C* **87**, 035503 (2013).  
 [3] S. Pastore, R. B. Wiringa, S. C. Pieper, and R. Schiavilla, *Phys. Rev. C* **90**, 024321 (2014).  
 [4] R. B. Wiringa and R. Schiavilla, *Phys. Rev. Lett.* **81**, 4317 (1998).  
 [5] A. Lovato, S. Gandolfi, R. Butler, J. Carlson, E. Lusk, S. C. Pieper, and R. Schiavilla, *Phys. Rev. Lett.* **111**, 092501 (2013).  
 [6] R. Schiavilla and R. B. Wiringa, *Phys. Rev. C* **65**, 054302 (2002).  
 [7] R. B. Wiringa, R. Schiavilla, S. C. Pieper, and J. Carlson, *Phys. Rev. C* **89**, 024305 (2014).  
 [8] R. Schiavilla, R. B. Wiringa, S. C. Pieper, and J. Carlson, *Phys. Rev. Lett.* **98**, 132501 (2007).  
 [9] P. Barreau *et al.*, *Nucl. Phys.* **A402**, 515 (1983).

[10] J. Jourdan, *Nucl. Phys.* **A603**, 117 (1996).  
 [11] R. B. Wiringa, V. G. J. Stoks, and R. Schiavilla, *Phys. Rev. C* **51**, 38 (1995).  
 [12] S. C. Pieper, *AIP Conf. Proc.* **1011**, 143 (2008).  
 [13] J. Carlson and R. Schiavilla, *Phys. Rev. Lett.* **68**, 3682 (1992).  
 [14] J. Carlson and R. Schiavilla, *Phys. Rev. C* **49**, R2880 (1994).  
 [15] R. Bryan, *Eur. Biophys. J.* **18**, 165 (1990).  
 [16] M. Jarrell and J. Gubernatis, *Phys. Rep.* **269**, 133 (1996).  
 [17] A. Lovato, S. Gandolfi, J. Carlson, S. C. Pieper, and R. Schiavilla, *Phys. Rev. C* **91**, 062501 (2015).  
 [18] F. Close, R. Roberts, and G. Ross, *Phys. Lett.* **129B**, 346 (1983).  
 [19] J. V. Noble, *Phys. Rev. Lett.* **46**, 412 (1981).  
 [20] I. C. Cloët, W. Bentz, and A. W. Thomas, *Phys. Rev. Lett.* **116**, 032701 (2016).  
 [21] S. Strauch *et al.*, *Phys. Rev. Lett.* **91**, 052301 (2003).  
 [22] O. Benhar, V. R. Pandharipande, and I. Sick, *Phys. Lett. B* **410**, 79 (1997).  
 [23] O. Benhar, V. R. Pandharipande, and I. Sick, *Phys. Lett. B* **469**, 19 (1999).  
 [24] O. Benhar and I. Sick, [arXiv:1207.4595](https://arxiv.org/abs/1207.4595).  
 [25] R. Schiavilla, O. Benhar, A. Kievsky, L. E. Marcucci, and M. Viviani, *Phys. Rev. Lett.* **94**, 072303 (2005).  
 [26] D. H. Lu, K. Tsushima, A. W. Thomas, A. G. Williams, and K. Saito, *Phys. Rev. C* **60**, 068201 (1999).  
 [27] P. A. M. Guichon and A. W. Thomas, *Phys. Rev. Lett.* **93**, 132502 (2004).  
 [28] M. W. Paris and V. R. Pandharipande, *Phys. Rev. C* **62**, 015201 (2000).  
 [29] J. Carlson, *Phys. Rev. C* **36**, 2026 (1987).  
 [30] J. Carlson, J. Jourdan, R. Schiavilla, and I. Sick, *Phys. Rev. C* **65**, 024002 (2002).  
 [31] F. Ajzenberg-Selove, *Nucl. Phys.* **A506**, 1 (1990).  
 [32] A. Nakada, Y. Torizuka, and Y. Horikawa, *Phys. Rev. Lett.* **27**, 1102 (1971).  
 [33] A. Nakada, Y. Torizuka, and Y. Horikawa, *Phys. Rev. Lett.* **27**, 745 (1971).  
 [34] M. Chernykh, H. Feldmeier, T. Neff, P. von Neumann-Cosel, and A. Richter, *Phys. Rev. Lett.* **105**, 022501 (2010);  
 [35] See Supplemental Material at <http://link.aps.org/supplemental/10.1103/PhysRevLett.117.082501> for the fitting procedure followed to extract the longitudinal transition form factors from the experimental data is illustrated. In addition, the explicit expressions for the electromagnetic currents employed in the calculation are given, which includes Refs. [36–39].  
 [36] L. E. Marcucci, M. Viviani, R. Schiavilla, A. Kievsky, and S. Rosati, *Phys. Rev. C* **72**, 014001 (2005).  
 [37] J. Carlson and R. Schiavilla, *Rev. Mod. Phys.* **70**, 743 (1998).  
 [38] C. E. Carlson, *Phys. Rev. D* **34**, 2704 (1986).  
 [39] J. Carlson, V. Pandharipande, and R. Schiavilla, in *Modern Topics in Electron Scattering*, edited by B. Frois and I. Sick (World Scientific, Singapore, 1991).  
 [40] J. B. Flanz, R. S. Hicks, R. A. Lindgren, G. A. Peterson, A. Hotta, B. Parker, and R. C. York, *Phys. Rev. Lett.* **41**, 1642 (1978).  
 [41] S. Karataglidis, P. Halse, and K. Amos, *Phys. Rev. C* **51**, 2494 (1995).  
 [42] A. Lovato, S. Gandolfi, J. Carlson, S. C. Pieper, and R. Schiavilla, *Phys. Rev. Lett.* **112**, 182502 (2014).  
 [43] C. Adams *et al.* (LBNE Collaboration), [arXiv:1307.7335](https://arxiv.org/abs/1307.7335).